MICS JOURNAL

Mathematics-in-Industry Case Studies Journal, Volume 2, pp. 16-33 (2010)

Mathematical and Numerical Modeling of the AquaBuOY Wave Energy Converter

Wacher, A. * Neilsen, K. †

Abstract. This paper presents the mathematical modeling and numerical methodology performed prior to the prototype deployment of the AquaBuOY, one of the few wave energy devices that have reached the ocean deployment stage. The combination of numerical computations, and laboratory testing produced some encouraging findings about how the AquaBuOY responds to real wave conditions. However, it also highlighted deficiencies in some of the early modeling, which emphasized the need for a time domain model in realistic wave conditions that includes accurate hydrodynamic and drag coefficients. This paper focuses on the governing equations that model the vertical dynamics of the AquaBuOY and the numerical solutions of these equations in order to predict the absorbed power of the device. Numerical results are presented in the time domain for both regular and irregular wave regimes (realistic wave conditions) as well as compared to experimental data in a regular wave regime.

While the two body system is challenging to model, due to the inclusion of variables such as the wave forcing term as well as identifying the non linear damping term along with a linear spring term needed to model the power takeoff system, it does provide a robust tool for wave energy research.

Keywords. Wave energy, Industrial mathematical modeling

1 Introduction

The world energy demand is increasing at an alarming rate, and producing electricity from alternative or renewable energy sources is becoming a necessity. Most governments are setting ambitious targets, which cannot currently be met with existing technologies. It is therefore crucial to find cost effective ways to harness energy from clean and sustainable sources. The offshore renewable energy sector is seeing a drastic increase in its activities. Wave, current, tidal and offshore wind

*Department of Mathematical Sciences, Durham University, Durham, DH1 3LE, United Kingdom abigail.wacher@durham.ac.uk

†Rambøll Denmark, Bredevej 2, 2830 Virum, Denmark kin@ramboll.dk

are topics that have been under academic investigation for decades, but have seen a recent influx in significant industry and venture capital funding. Harnessing the power of the wave is not a recent endeavor. In the late 1860's, Robertson constructed the first wave-power boat [10]. It was not a complete success, but over the last century, engineers and inventors have focused on ocean powered technologies. For examples see [1]. Recently the focus of most programs has been in the conversion of wave energy into electricity; even though desalinization and energy storage are often mentioned as well. Wave energy devices are often categorized into the following major groups.

- Point absorber
- Attenuator (surface follower)
- Terminator
- Oscillating water column
- Overtopping

The physics of power absorption amongst the variety of devices is very different, however other devices and descriptions are outside the scope of this paper. It should be noted however that the AquaBuOY is a prime example of a point absorber.

This paper focuses on describing the physical device and the mathematical modeling that was performed to predict the power performance in both operational and extreme sea states. Operational sea states are important from an economic standpoint. Being able to have an accurate prediction of power generation is key to understanding the viability of a farm. Expected revenues and wave farm capital and operational expenses are very valuable data to have in validating a wind farm development business plan. Extreme sea state motion and load prediction are very important to the designer, to ensure that the device will not fail in large storms.

The scope of this paper is to present a mathematical model of the vertical dynamics of the AquaBuOY which is used to obtain numerical predictions of the absorbed power of the device. The main model described here is used as a tool to optimize the wave energy extraction from a particular device. These numerical tools are used prior to physically building prototypes which can be very expensive. They are also used in the optimization of the devices, since sensitivity studies are performed signifncatly faster on a computer than in a lab. However, having confidence in the numerical tools is crucial. Therefore the validation of the tool is often performed at a small scale, in a lab, where the environment can be controlled.

In the case of the AquaBuOY, the numerical tools were developed, then a campaign of model tests was conducted at the Hydraulics and Maritime Research Centre (HMRC), in Ireland. At the end of the model test campaign, the decision was made to install a prototype in Oregon, to test a 1:2 scale prototype, in real ocean conditions.

The AquaBuOY, shown in figure 1. consists of a floater, which provides buoyancy to the system and keeps it afloat. Connected underneath the floater is a large cylinder, called the accelerator

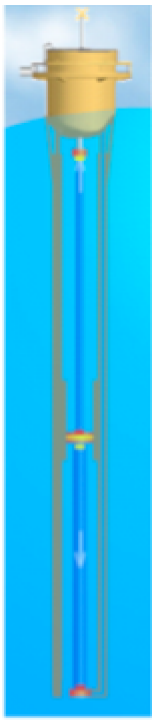

Figure 1: *Schematic of the AquaBuOY.*

tube. It is open to the ingress of water on both sides, however a piston resides in the center of the accelerator tube and is connected to the top and the bottom section of the buoy using a hose pump, made of a semi elastic material. The natural frequencies of the piston and the buoy differ by design, resulting in significant relative motions between the two, stretching or compressing the hose pump. Water in the pump is being pushed, though a system of check valves, through a hydraulic system which terminates into a Pelton turbine. This turbine directly generates electricity. The hose pump system here forth is referred to as the Power Takeoff (PTO) system.

The results from the numerical model discussed in this paper compared well to the actual buoy design at a fiftieth scale (results at the fiftieth scale are scaled up to full scale for comparison). Similar results were obtained for the half scale buoy (deployed in 2007 off of the coast of Oregon, USA) though none of these comparisons are included in this paper. The numerical results are extensive and are not discussed thoroughly in this paper, but will be the focus of a follow -on publication geared towards the ocean energy community in due time if the results are released. However, we will show some results from the numerical model of a theoretical full scale buoy in both regular and irregular wave regimes as examples of the results that are used in the optimization process. We also present one sample of results for average power absorbed from the numerical time domain model discussed in this paper compared to physical fiftieth scale lab results scaled up to full scale. For the interested reader see related papers [7] and [8].

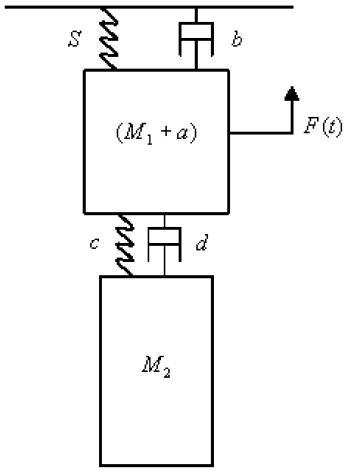

Figure 2: *Mass spring system modeling the AquaBuOY vertical dynamics.*

2 Model equations

The vertical dynamics of the AquaBuOY is modeled as a two-body system (see figure 2) including a float connected to the submerged mass (PTO - hose pump system). Only the vertical dynamics are considered in this model since the AquaBuOY is designed such that the water line is at the buoy and the center of gravity is below the buoy, in order to keep the AquaBuOY vertical. First we will define the variables for a reduced set of model equations corresponding to figure 2. Then we will proceed in the following subsections to explain some of the terms more in depth, as well as adding the necessary complexity to the terms. Please refer to section 7 for a table of the relevant nomenclature used throughout this paper (including those defined below).

- M_1 is the structural mass of the float. This is calculated from the float water plane area (A_w), float draft (h_f) and density of the water (ρ).
- a is the added mass of water for the float. In fluid mechanics, added mass is the inertia added to a system since an accelerating or decelerating body must move some volume of surrounding fluid as it moves through it. The implementation of this coefficient is discussed in more depth in section 2.2.
- b is the hydrodynamic damping of the float (sometimes called viscous damping). The force a body is subjected to from simple harmonic motion at very small amplitudes and high frequencies in water due to excitations that come from outside. The implementation of this coefficient is discussed in more depth in section 2.2.
- $S = S_{hs}$ is the hydrostatic stiffness parameter (sometimes called the restoring force, see [12]). This is calculated from the float water plane area and the density of the water.

- d is the damping of the PTO system. The AquaBuOY design discussed in this paper has a non linear damping term which is discussed in more detail in section 2.5.

- c is the PTO spring stiffness. This coefficient is measured in the lab for the particular hose pump specifications.

- F_w is the wave exciting force (see section 2.1). The wave exciting force can be from a regular wave regime (discussed in section 2.1.1) which is unrealistic in ocean waves, though it is reproducible in the lab environment for testing. The wave exciting force can also be from an irregular wave regime (discussed in section 2.1.2) which is a more realistic model of ocean waves.

- M_2 is the mass of the water in the accelerator tube calculated from the accelerator tube length (L_t) and diameter (D_t), and the water density.

- z_1, $\dot{z}_1$ and $\ddot{z}_1$are the float displacement, velocity and acceleration (measured from its initial values).

- z_2, $\dot{z}_2$ and $\ddot{z}_2$ are the piston displacement, velocity and acceleration (measured from its initial values).

Applying D'Alembert's law that the sum of all forces acting on a body (for each mass) is equal to zero, we obtain the following system of linear second order ordinary differential equations corresponding to the vertical motion of the two bodies in figure 2.

$$\begin{aligned} (M_1 + a)\ddot{z}_1 + b\dot{z}_1 + S_{hs}z_1 + d(\dot{z}_1 - \dot{z}_2) + c(z_1 - z_2) &= F_w(t) \\ M_2\ddot{z}_2 = d(\dot{z}_1 - \dot{z}_2) + c(z_1 - z_2) & \end{aligned} \tag{1}$$

So far this formulation of the problem ignores the hydrodynamic forces on the mass of water in the tube and ignores any friction and drag between the water and the the frame or body of the buoy (hull).

The system (1) can be solved analytically in the frequency domain when considering the regular wave regime, however as the frequency domain results have been presented in many books for a one-body problem with linear damping, the interested reader is referred to [3]. Since we are truly interested in the irregular wave regime it is necessary to solve these equations in the time (t) domain, thus we cannot rely on the analytic (regular wave regime) solutions beyond obtaining very rough approximations. However the analytic solutions can be used for validating time domain models when the irregular waves are replaced with regular waves (and in the case of the AquaBuOY when the non linear damping, discussed shortly, is replaced with a linear damping term).

2.1 Wave exciting force

The wave exciting force F_w in the system of differential equations is a function of time, both for regular waves and for irregular waves. The theory describing what is involved in modeling the term F_w discussed following can be found in [6]. For regular waves (known as monochromatic waves or harmonic waves) the wave exciting force can be calculated analytically for a particular wave amplitude ($A_{wave} = H/2$, where H is defined as the wave height), and for a particular wave period T or rather for the corresponding frequency $\omega = 2\pi/T$. In section 2.1.2 it is outlined how we obtain a wave exciting force in a random or irregular sea (panchromatic waves) for some average wave period T_z. The latter is a more realistic model of the waves in the ocean since these are waves formed by a composition of waves of different frequencies.

2.1.1 Wave exciting force for regular waves

Assuming monochromatic waves we can define the wave exciting force as a function of time as

$$F_w(t) = A_{wave}F(\omega)cos(\omega t + \gamma), \tag{2}$$

where the wave amplitude is $A_{wave} = H/2$, γ is the phase difference between the wave and the force (we set $\gamma = 0$), and the cyclic frequency $\omega = 2\pi/T$.

2.1.2 Wave exciting force for irregular waves

We now look at a wave super-imposed by many regular waves of different heights and periods, which models the irregular wave patterns in a random or irregular sea (see [2] for further details of the material discussed following in this section). The height of each wave component is guided by the *Wave Energy Density Spectrum*, usually just referred to as the wave spectrum.

The spectrum is a function that defines how much energy is contained in each frequency of the wave. Based on real sea measurements a number of generic spectrum have been proposed to describe how the energy is distributed. In nature one can measure the waves over say 20 minutes and from the measured time series determine what is the average wave period and the significant wave height. To reproduce an irregular wave with the same significant wave height and average period one can use the PM spectrum as defined below.

The wave conditions in a particular location in the sea are described in terms of the significant wave height H_s and the average wave period T_z. It has been found by [9] that the period corresponding to the peak of the wave energy spectrum T_p is related to the average wave (zero-crossing) period T_z by

$$T_p = 1.4T_z. \tag{3}$$

The panchromatic spectrum described following can be defined from H_s and T_z given the relation (3) (see [2]).

PM-spectrum (H_s and T_p) The spectrum we describe following is the Bretchsneider spectrum, but in view of its general similarity in shape compared to the PM spectrum it is referred to as the PM spectrum, named after two researchers Pierson and Moscowitz that derived a spectrum $S(f)$ (where the frequency $f = 1/T$), from numerous studies and measurements at sea as:

$$S(f) = \frac{A}{f^5} \exp(-\frac{B}{f^4}). \tag{4}$$

To generate specified sea conditions two parameters are given to determine the shape of the spectrum:

- The peak period T_p.
- The significant wave height H_s.

The value A is then determined from the desired significant wave height H_s and desired peak frequency $f_p = 1/T_p$, and B depends on the peak frequency alone as:

$$A = \frac{5H_s^2 f_p^4}{16}, \tag{5}$$

$$B = \frac{5f_p^4}{4}. \tag{6}$$

The spectrum is then composed of a set of N frequencies, with components f_i. Each frequency is calculated as:

$$f_i = \frac{\triangle f \cdot \text{rand}(1)}{2} + i \cdot \triangle f \tag{7}$$

where $\triangle f = 0.01$, rand(1) is a random number between 0 and 1, and $i = 0, ..., N-1$. Using a randomly chosen number rand(1) for each frequency in this way, means that the interval between each frequency is not constant. This means that the time series does not repeat itself as it would with constant steps. The amplitude of each wave component is then given by

$$a_i = \sqrt{2S(f_i)\triangle f}, \tag{8}$$

with a corresponding random phase

$$\phi_i = 2\pi \cdot \text{rand}(1). \tag{9}$$

The force signal is then calculated at any time t by multiplying each wave component with the wave exciting force amplitude (at unit wave amplitude):

$$F_w(t) = \sum_{i=0}^{N} \left[a_i \sin(2\pi f_i t + \phi_i) F(1/f_i) \right]. \tag{10}$$

2.2 Added mass and hydrodynamic damping

The variables a and b for the added mass and the hydrodynamic damping are unique to each particular AquaBuOY shape for a given array of periods T. The models and tools used for obtaining these coefficients falls under the area of hydrodynamics. We use a software package called WAMIT (a frequency domain commercial software which generates hydrodynamics coefficients such as wave exciting forces and drift forces using a boundary element method) to obtain the hydrodynamic parameters for the AquaBuOY. For the model of this paper the parameters needed are the added-mass a, the damping coefficient b, and the exciting force F (for unit amplitude, used in the formulations discussed in section 2.1). One can however also implement their own hydrodynamic code to obtain these coefficients if time is not a constraint.

For the given shape of the buoy (of which the specifications are not included in this paper), and a given array of periods T, WAMIT produces corresponding arrays for the values of a, b and the excitation force F (at unit amplitude). The given data is non-dimensional and scaled. Note that the hydrodynamics considered here are for the interaction of the water and the exterior of the buoy attached to the accelerator tube. That is, the motion of the piston inside of the accelerator tube shown in figure 1 and modeled in this paper is immaterial to obtaining the hydrodynamic parameters a, b and F, though we need these parameters to then obtain the motion of the piston via the model described in this paper.

From theory (see [4]) we know that in the system of equations (1) we can replace the added mass a by the average added mass, and the term bv_1 can be replaced by the following integral:

$$\int_{-\infty}^{t} h(t-\tau)v_1(\tau)\mathrm{d}\tau, \tag{11}$$

where the retardation function $h(\tau)$ (see [4] and [5]) is defined as

$$h(\tau) = \frac{2}{\pi}\int_0^{\infty} b(\omega)cos(\omega\tau)\mathrm{d}\omega. \tag{12}$$

This replacement is valid for both regular waves and irregular waves, however it is mostly useful for irregular waves since at each time the irregular wave exciting force (see equation (10)) is composed from different wave periods which means that we would need to interpolate the corresponding a and b at each step in time. However with the added mass replaced by its average value (since the added mass does not change very much) and the term bv_1 replaced by the integral in (11) (which is approximated by a sum described following), these values need not be calculated (interpolated from WAMIT data for a given set of wave periods) at each time step. The integral in (11) is approximated using a standard quadrature rule as follows

$$\int_{-\infty}^{t} h(t-\tau)v_1(\tau)\mathrm{d}\tau = \sum_{n=1}^{N}(h(n\mathrm{d}t)v_1(t-n\mathrm{d}t)\mathrm{d}t) + \frac{1}{2}h(0)v_1(t)\mathrm{d}t, \tag{13}$$

noting that only the first N ($N = 40$ say) terms are included in the sum since the trailing terms of the retardation function are close to zero.

The added mass is calculated as

$$a_\infty = a(\omega) + \frac{1}{\omega}\int_0^\infty h(\tau) sin(\omega\tau) \mathrm{d}\tau, \tag{14}$$

and since this value doesn't have much variation within the frequencies we are interested in ($\omega = 0.5$ and $\omega = 2$ for modeling in realistic ocean conditions), the average value is used.

2.3 Fluid friction (drag)

In fluid dynamics, drag (sometimes called fluid resistance or fluid friction) refers to forces that oppose the relative motion of an object through a fluid. To include fluid friction (see [11]) we add to the left hand side of the first equation in the system of ODEs (1), the term:

$$F_{ff} = A_w C d \rho |v_1| v_1, \tag{15}$$

where Cd is a measured coefficient (a value which falls between 1 and 2 for the particular AquaBuOY shape).

2.4 Force and Power

In the case of linear damping $d = b_2$ in the system of equations (1), the PTO force F_{pto} $[N]$ is derived as:

$$F_{pto} = b2(v_1 - v_2) + c(z_1 - z_2), \tag{16}$$

or defining the extension $z_r = (z_1 - z_2)$ and the extension velocity (or relative velocity) by $v_r = (v_1 - v_2)$ as

$$F_{pto} = b_2 v_r + c z_r. \tag{17}$$

In practice, in order to obtain the linear damping b_2 from a physical model, one graphs the force versus the relative velocity. The slope of the graph is b_2.

The absorbed power P_{abs} $[Watts]$ in the PTO system is in general the force times the velocity

$$P_{abs} = F_{pto} v_r = b_2 v_r^2 + c z_r v_r. \tag{18}$$

In the case of non-linear damping which characterizes AquaBuOY, we describe the expression for Force and Power in the following section. For a good reference about general wave energy extraction modeling see [3].

2.5 Non-linear damping

The equations discussed so far have been modeling a system with linear damping. However, the model of the hose pump is not linear and a good approximation can be obtained by combining a linear spring (with spring stiffness c) with Coulomb damping. The Coulomb damping gives a constant force opposing the direction of the motion, this would be

$$F_{pto} = F_{fric} sign(v_1 - v_2) + c(z_1 - z_2), \tag{19}$$

where

$$sign(x) = \left\{ \begin{array}{lll} -1 & if & x < 0 \\ 1 & if & x > 0 \\ 0 & if & x = 0 \end{array} \right\}. \tag{20}$$

This means that if the relative velocity becomes zero, the acceleration force from the water in the tube must overcome the PTO force (which then depends on the position of the piston). In order to obtain the damping coefficient F_{fric} from a physical model, one graphs force versus extension (which is a trapezoidal graph) and takes the difference between the upper line and the lower line, divided by two.

To include the non-linear Coulomb damping the only change that needs to be made in the system (1) is to replace the term

$$b2(v_1 - v_2) \tag{21}$$

by the term

$$F_{fric} sign(v_1 - v_2). \tag{22}$$

3 Numerical implementation

The following is a brief overview of how these equations are solved in the time domain for regular and irregular waves including the non linear damping of the AquaBuOY. However a similar approach may be applied to other point absorber wave energy devices corresponding to different power takeoff systems. The time varying model was implemented in MATLAB and validated against earlier Simulink irregular wave models (Simulink is a MathWorks product. It is an environment for multidomain simulation and Model-Based Design for dynamic and embedded systems).

The benefit of solving these equations using a high level programming language, such as MATLAB, for solving these equations is optimization. When designing such a complex system such as a wave energy device, even for point absorber devices which are not the most complex, the aim is to maximize the energy output. It is also important to minimize the cost (and sometimes the size) of

the device. These goals require a large number of simulations due to the vast amount of variables that can be modified for an optimal design.

In order to solve a system such as (1) using the built in MATLAB ODE solver packages we convert the second order differential equations into a system of first order differential equations. We follow a standard change of variables to reduce the order of the ordinary differential equations. We introduce the variables $v_1 = \dot{z_1}$ and $v_2 = \dot{z_2}$. The second order system of ordinary differential equations in (1) can then be rearranged, letting $\mathbf{y} = (z_1, z_2, v_1, v_2)^T$ and $\dot{\mathbf{y}} = (\dot{z}_1, \dot{z}_2, \dot{v}_1, \dot{v}_2)^T$ resulting in a system written as

$$\dot{y} = f(y), \tag{23}$$

where $f(y)$ is the "right hand side" resulting from the rearrangement of the system of equations in (1) but including the retardation function and average added mass formulations from section 2.2, the fluid friction from section 2.3, the regular or irregular wave exciting force formulations from section 2.1 and the non linear damping from section 2.5.

In the implementation of the model described, the function $sign(x)$ in section 2.5 is replaced with $tanh(100x)$. The function $tanh(100x)$ satisfies the same conditions as $sign(x)$ however it transitions between 1 and -1 smoothly. This replacement is made in order to avoid the singularities in the system of ODEs, which result in numerical instabilities. Other techniques of course can also be used to avoid these singularities.

The system (23) together with the zero dirichilet initial conditions for each of z_1, z_2, v_1 and v_2, form the system of equations which are solved for the unknown displacements and velocities as functions of time. Though this system can be solved using any number of standard ODE solvers, we have chosen to use MATLAB's stiff ode solver ode15s due to the stiffness of the system of equations. We note however that MATLAB's ode45 was sufficient for solving the equations with linear damping in a regular wave regime.

It should be noted that for some of the input variables, in particular those regarding the shape of the buoy, we needed to reproduce the hydrodynamic parameters a, b and F using WAMIT in order to then produce the dynamics results using the model discussed in this paper. We note that in WAMIT the tube is modeled using a "thicknessless" element, so it has no buoyancy contribution.

For a fixed buoy shape many variables can be changed directly within this model without the need to reproduce the hydrodynamic parameters using WAMIT. The most widely varying parameters are the wave heights and wave periods for a particular ocean (and in the case of validation for a large series of wave tank experiments). The effects from varying the non linear damping and spring stiffness coefficients were also examined without the need to reproduce the hydrodynamic input data.

4 Numerical solutions of the model within regular and irregular wave regimes

Figure 3 shows the displacements z_1, z_2 (from the initial positions) for the float and the piston respectively, as well as the relative displacement in a regular wave regime. To obtain these solutions we used the excitation force defined in equation (2). The results shown in figures 3,4 and 5 are obtained using the full scale buoy specifications (though the actual specifications are not included in this paper due to proprietary reasons) in the regular wave regime with wave period $T = 10.2s$ and wave height $H = 2.5m$. These types of solutions have been used for validation, such as validating the force as a function of time and extension (similar to what is shown in figure 4) of the actual hose pump laboratory experiments. Also the solutions shown in figure 5 are used for approximations of absorbed power assuming the average wave height and period are used as the wave height and period for a regular wave regime.

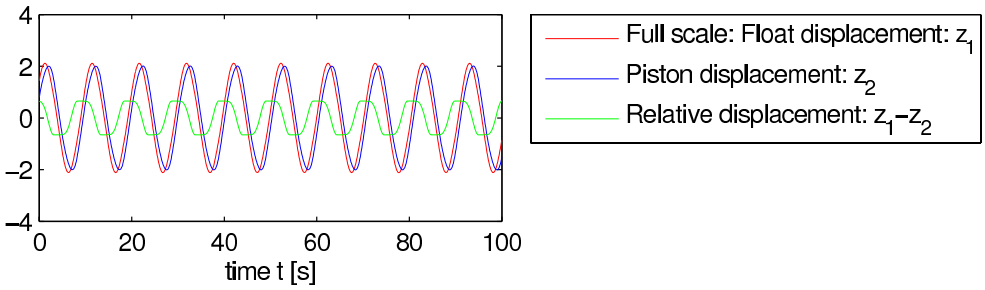

Figure 3: *Solutions of displacement in a regular wave regime. Displacement is measured in meters [m].*

In figures 6, 7 and 8 we show results of a half scale buoy configuration in an irregular wave regime (see equation (10)) with an average wave period $T_z = 5.5s$ and a significant wave height $H_s = 3m$. The solutions shown in figure 6 for the displacements of the buoy, the piston and the relative displacement are very different than shown in figure 3 and are included here to display what the solutions of motion of the AquaBuOY look like in a more realistic wave regime. The results from this model compared very well with the actual data processed from the half scale AquaBuOY in 2007 as well as the fiftieth scale model of the AquaBuOY tested in Cork, Ireland in 2006 and 2007 (the experimental results for the half scale were not released by Finavera at this time due

to proprietary reasons). The time scale for the solutions in the irregular wave regime is about 10 times that for the regular wave regime solutions due to the fact that the amount of time for the average absorbed power (see figures 5 and 8) to converge to a steady value is tenfold in the irregular wave regime as compared to the regular wave regime. This expediency is one of the reasons that regular wave regime models can be useful initially. The graphs of the forces are also interesting to note, when comparing the results from a regular and irregular wave regime. In figure 7 it is clear that under more realistic conditions, the force (as a function of extension of the hose pump) is not a perfect quadrilateral but rather has some data scattered inside the outline of a quadrilateral. While the results obtained for force in a regular wave regime were used in the earlier stages to compare the hose pump failure tests, the results obtained in the irregular wave regime were much more realistic and fit much better to the actual hose pump data.

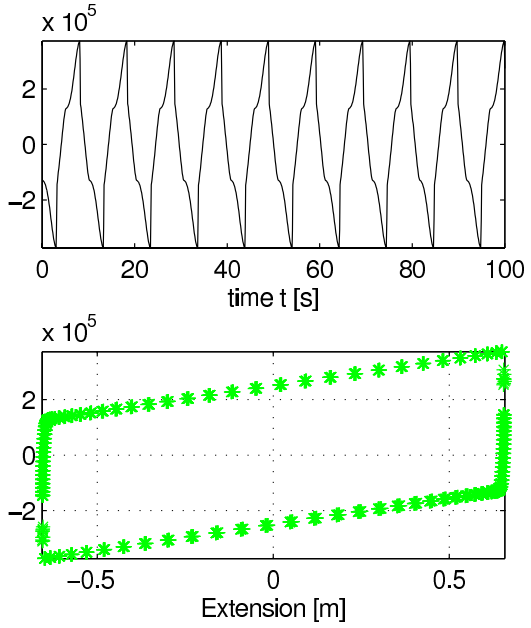

Figure 4: *The force in the power take off system is calculated using the solutions of displacement in a regular wave regime. The top graph shows the force as a function of time. The bottom graph shows the force as a function of extension. Force is measured in Newtons [N].*

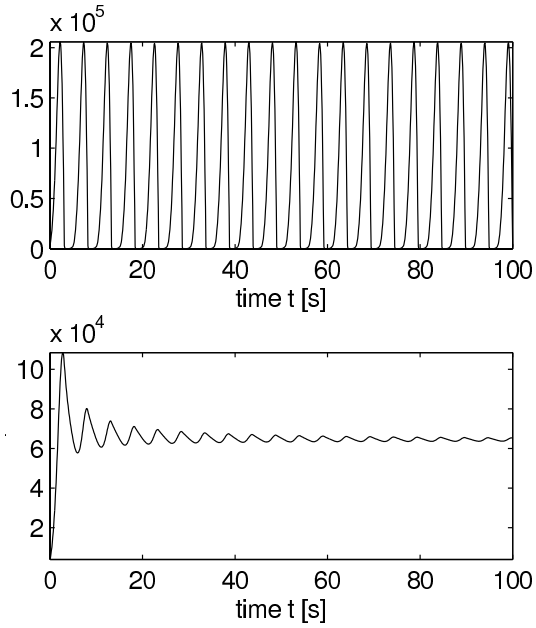

Figure 5: *The power in the power take off system is calculated using the solutions of velocity and force in a regular wave regime. The top graph shows the power as a function of time. The bottom graph shows the power as a running average function over time. Power is measured in Watts [W].*

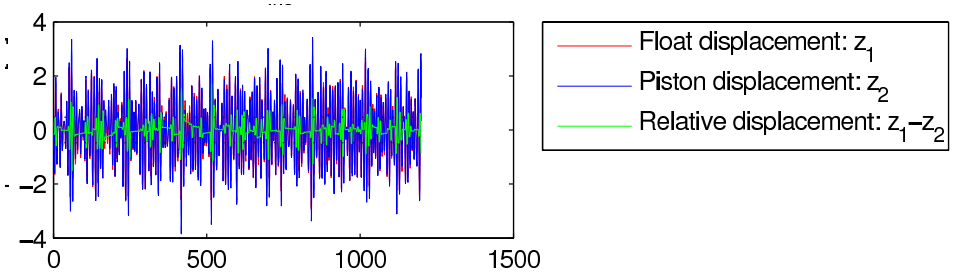

Figure 6: *Solutions of displacement in an irregular wave regime. Displacement is measured in meters [m].*

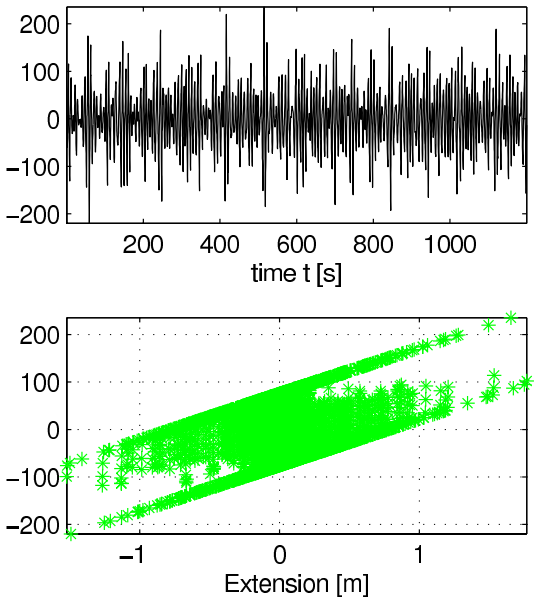

Figure 7: *The force in the power take off system is calculated using the solutions of displacement in an irregular wave regime. The top graph shows the force as a function of time. The bottom graph shows the force as a function of extension. Force is measured in Kilonewtons [kN].*

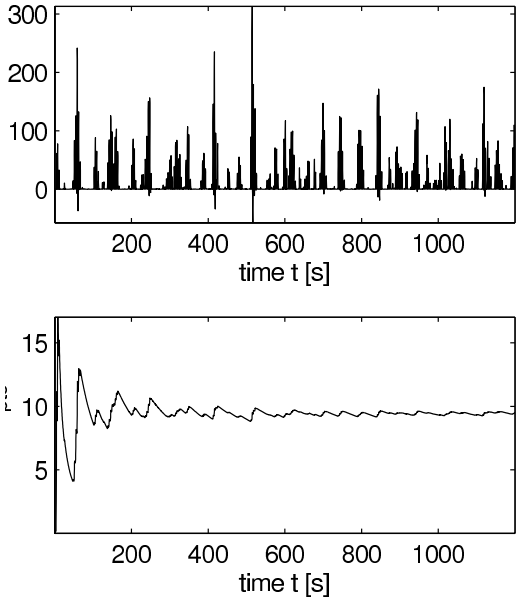

Figure 8: *The power in the power take off system is calculated using the solutions of velocity and force in an irregular wave regime. The top graph shows the power as a function of time. The bottom graph shows the power as a running average function over time. Power is measured in Kilowatts [kW].*

5 Physical model results compared to numerical solutions

Figure 9 shows a comparison of results in a regular wave regime, including a set of numerical solutions for average power in the time domain and the corresponding experimental results for the 1:50 scale model tested at HMRC, Ireland. The numerical results in the time domain were evaluated for the dimensions of the model at the full scale (chosen by the engineering team at the time of prototype design). Everything in the 1:50 scale experimental results was scaled up to the full dimensions according to Froude scaling, using a ratio of 1:50. We note that the comparison of results from the 1:50 scale physical model scaled up to prototype scale for comparison is not ideal for particular comparisons, however due to the large number of results produced due to lab experiments at several different scales, the engineering team at the time of this research chose to stick with a single prototype reference and any experiments from all scales would be scaled up to prototype in order to analyze and as well for the numerical comparisons. The HMRC results at the 1:50 scale are correct in the motion and power prediction. However these tests were performed at a relatively small scale in the lab and some quantities, such as viscous damping do not scale well and usually cause conservative results as is shown in figure 9.

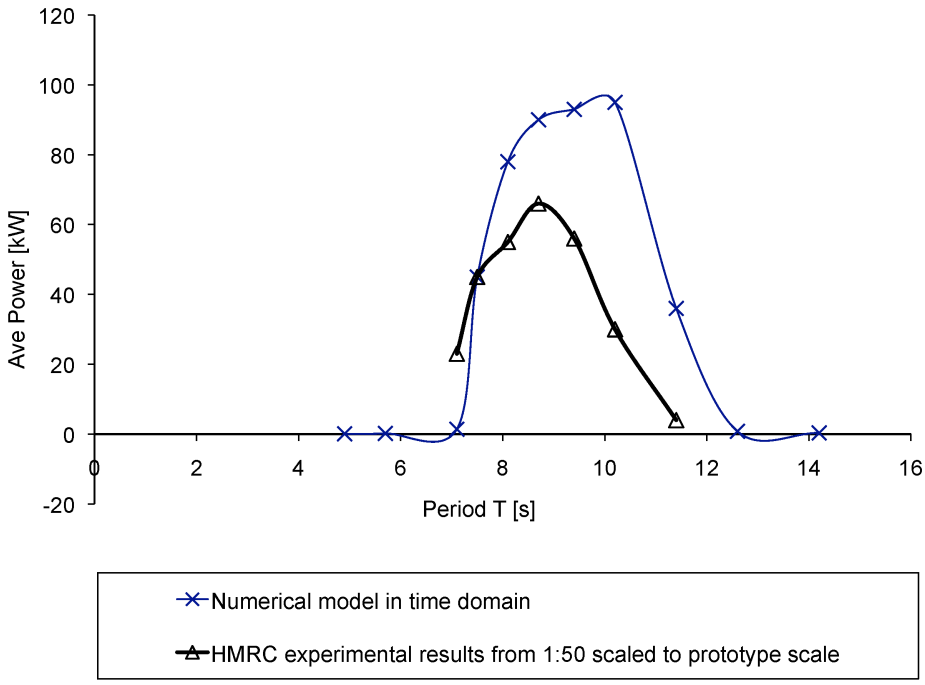

Figure 9: *Average power output in a regular wave regime.*

6 Conclusions

We have introduced a mathematical model of the vertical dynamics of the AquaBuOY's buoy and hose pump power take off system. The numerical results captured the physics of the AquaBuOY

experimental results at the fiftieth scale. Though the half scale results are not included in this paper, due to proprietary reasons, it can be reported that these also reproduced the physics of the AquaBuOY. The numerical implementation of the model is extremely fast for the regular wave regime (seconds) and nearly real time for the irregular wave regime, which are more useful as they are more realistic than regular waves. The tool developed for this study was useful in the optimization studies for the design of the AquaBuOY half scale, however future work is recommended for implementing an optimized time integration scheme to solve the ordinary differential equations, particularly in the irregular wave regime, as it would be useful to make the optimization faster. The numerical model has proved to be robust, efficient and useful.

7 Nomenclature

Definition	Label	Units
Period (for regular waves)	T	$[s]$
Wave height (for regular waves)	H	$[m]$
Average wave period (for irregular waves)	T_z	$[s]$
Significant wave height (for irregular waves)	H_s	$[m]$
Wave exciting force	$F_w(t)$	$[N]$
Water density	ρ	$[kg/m^3]$
Acceleration due to gravity	$g = 9.81$	$[m/s^2]$
Float diameter	D	$[m]$
Float draft	h_f	$[m]$
Float water plane area	$A_w = (\pi/4)D^2$	$[m^2]$
Structural mass of float	$M_1 = A_w h_f \rho$	$[kg]$
Hydrostatic stiffness parameter	$S_{hs} = A_w \rho g$	$[N/m]$
Tube length	L_t	$[m]$
Tube diameter	D_t	$[m]$
Mass of water in accelerator tube	$M_2 = (\pi/4)L_t \rho D_t^2$	$[kg]$
Added mass of water for float	a	$[kg]$
Hydrodynamic damping of float	b	$[Ns/m]$
PTO spring stiffness	c	$[N/m]$
Time	t	$[s]$
Damping coefficient	d	[Ns/m]
Linear damping ratio	cd	no units
Linear damping of relative motion	$b_2 = cd\sqrt{S_{hs}M_1}$	$[Ns/m]$
Non-linear Coulomb damping (see eqn. (19))	F_{fric}	$[N]$

8 Acknowledgements

The first author would like to thank the CA-OE partners for supporting her training at the Hydraulics and Maritime Research Centre (HMRC), University College Cork. Further we would like to thank the Danish energy agency and energinet.dk for financial support towards the development of the system. We also would like to thank Dr. Dominique Roddier for providing the hydrodynamic data for which this model relied on.

References

[1] Evans, D.V., A theory for wave-power absorption by oscillating bodies, *Journal of Fluid Mechanics* **77** (1976), 1-25. 17

[2] Lloyd, A.R.J.M., *SEAKEEPING ship behaviour in rough weather*, Ellis Horwood Limited 1989. 21

[3] Falnes, J., *OCEAN WAVES AND OSCILLATING SYSTEMS Linear interactions including wave-energy extraction*, Cambridge University Press 2002. 20, 24

[4] Cummins, W. E., The impulse response function and ship motions, *Schiffstechnik* **9** (1962), 101-109. 23

[5] Ogilvie, T.F., *Recent progress toward the understanding and prediction of ship motions*, Proceedings of the 5th Symposium on Naval Hydrodynamics 1964. 23

[6] Newman, J.N., The exciting forces on fixed bodies in waves, *Journal of Ship Research* **6** (1962), 10-17. 21

[7] Mavrakos, S.A., Katsaounis, G.M., Nielsen, K., and Lemonis, G., *Numerical performance investigation of an array of heaving wave power converters in front of a vertical breakwater*, International Offshore and Polar Engineering Conference (ISOPE) 2004. 18

[8] Nielsen, K. and Smed, P.F., *Point absorber optimisation and survival testing*, Proceedings of the Third European Wave Energy Conference 1998. 18

[9] Hogben, N., Dacunha, N.M.C., and Olliver, G.F., *Global Wave Statistics*, British Maritime Technology 1986. 21

[10] The San Francisco self propelling boat -disastrous end of a grand experiment, *The New York Times* **7** (1868), May 10th. 17

[11] Newman, J.N., *Marine Hydrodynamics*, MIT Press 1977. 24

[12] Huang, L.L., and Riggs, H.R., The hydrostatic stiffness of flexible floating structures for linear hydroelasticity, *Marine Structures* **13** (2000), 91-106. 19